Procedures for Graphical Rectification Of TIROS Photographs

By
Gene Wooldridge

Project WISP
Report No. 3

Contract Cwb - 10879
with U. S. Department of Commerce,
Weather Bureau

Colorado State University
Atmospheric Science Technical Paper No. 71

August 1965

Colorado
State
University

Department of
Atmospheric Science

Paper No. 71

PROCEDURES FOR GRAPHICAL RECTIFICATION
OF TIROS PHOTOGRAPHS

by

Gene Wooldridge

Project WISP

Report No. 3

Colorado State University

Atmospheric Science Technical Paper No. 71

August 1965

LIST OF ILLUSTRATIONS

LIST OF TABLES

Procedures for Graphical Rectification of TIROS Photographs

by

Gene Wooldridge

Abstract

Graphical rectification procedures for TIROS photographs are reviewed and presented. An example of rectification of a tape mode orbit is performed, and the required steps individually shown. A graphical method is used for making time corrections for the tape mode. Simplified instructions of Fujita's <u>approximate</u> method are given and illustrated by drawings. Data sources and requirements, as well as chart requirements are listed. The accuracy necessary for meteorological research is retained while time requirements are considerably less than Fujita's <u>precise</u> method.

Introduction:

With the advent of TIROS satellite photography, a new and useful tool was made available to meteorology and related disciplines with which to gain increased understanding of the complex nature of the earth's atmosphere. Tens of thousands of useable photographs were taken by TIROS satellites, beginning with TIROS I on April 1, 1960 (Fritz, 1964). Numerical and graphical methods (Fujita, 1961, 1963, 1964) were developed by which grids of latitude and longitude lines could be superimposed on the photographs. From these grids cloud areas and configurations could be defined and studied.

From the first day of TIROS I operation it became clear that many details of cloud cover not discernible from the ground

because of sparsity of data or inadequacy of observations could be determined from the TIROS photographs. Investigators have studied cloud patterns in conjunction with conventional analyses and have been able to correlate specific cloud patterns with meteorological phenomena at the meso- and synoptic scales.

For optimum use, the photographs required very accurate photogrammetric analysis so that latitude and longitude lines could be placed on the photographs with an error tolerance of less than 10-20 miles. Automated methods of satellite attitude determination allowed rapid calculations to be made by means of high-speed computors, but data extracted, or graphically determined, from the pictures themselves remained the most reliable source of information (Goldshlak, 1963). Thus, the graphical methods developed by Fujita for both precise and approximate rectification have been used extensively in connection with research and operational use of TIROS photographs.

Since precise graphical analysis had proved time-consuming, a single rectification procedure was needed which retained the desired accuracy, but which could be more easily learned and carried out. Fujita's approximate method[1] accomplishes this by incorporating definitive satellite altitude data. The present report aims to simplify the step-by-step instructions, thus making them more easily applicable. The same grids and charts which Fujita developed are utilized.

SATELLITE CHARACTERISTICS

The TIROS satellites orbit about the earth approximately every 100 minutes, during which time the earth rotates about 25 degrees. Mounted in the satellites are television cameras whose optical axes lie approximately along the spin axis. On the vidicon of the television cameras are etched a center "crossed" fiducial mark and four

---

[1] Fujita, Tetsuya, 1963: A Technique for Precise Analysis for Satellite Data; Volume 1 - Photogrammetry. Meteorological Satellite Laboratory, Report No. 14.

"L-shaped" corner fiducial marks; the purpose of these marks is
to locate points so that grids may be constructed from which cloud
and / or ground features may be located.

The cameras are of three types: narrow angle, medium angle,
and wide angle lenses. The wide angle camera is most commonly
used, and has a field approximately 700 miles square, with a resolution
of 1.5 to 5 miles, depending on the angle of the optical axis with respect
to the local vertical. Figure 1 shows the relationship of the orbit,
the earth, the satellite, and the optical axis (terms used in Fig. 1
are explained in the glossary). The satellites carry a combination
of two of the three camera types. TIROS satellites I through IV
traveled orbits ranging between approximately 48 degrees north and
south, while TIROS V through VIII traveled between approximately
58 degrees north and south.

Although the spin axes of the satellites do not coincide exactly
with the optical axes, the nutation is generally small, and the axes
are taken to be the same for the purposes of rectification. Other
minor factors, such as the effects of different cloud heights and the
oblateness of the earth, are also ignored in the rectification pro-
cedures since the errors involved in these approximations are within
acceptable limits (Fujita, 1964).

The cameras may be programmed to take a total of 32 pictures,
with a camera shutter speed of 1.5 milliseconds. The readout is
either direct, when the satellite is within line of sight of the readout
station, or by delayed tape if not within line of sight at picture-taking
time. The time interval between pictures for direct readout is
generally 10 seconds, and for tape readout it is 30 seconds. The
picture-taking time for direct mode is assumed to coincide with the
programmed time, but errors often occur in the timing mechanism
for the tape mode so that the time at which pictures are actually taken
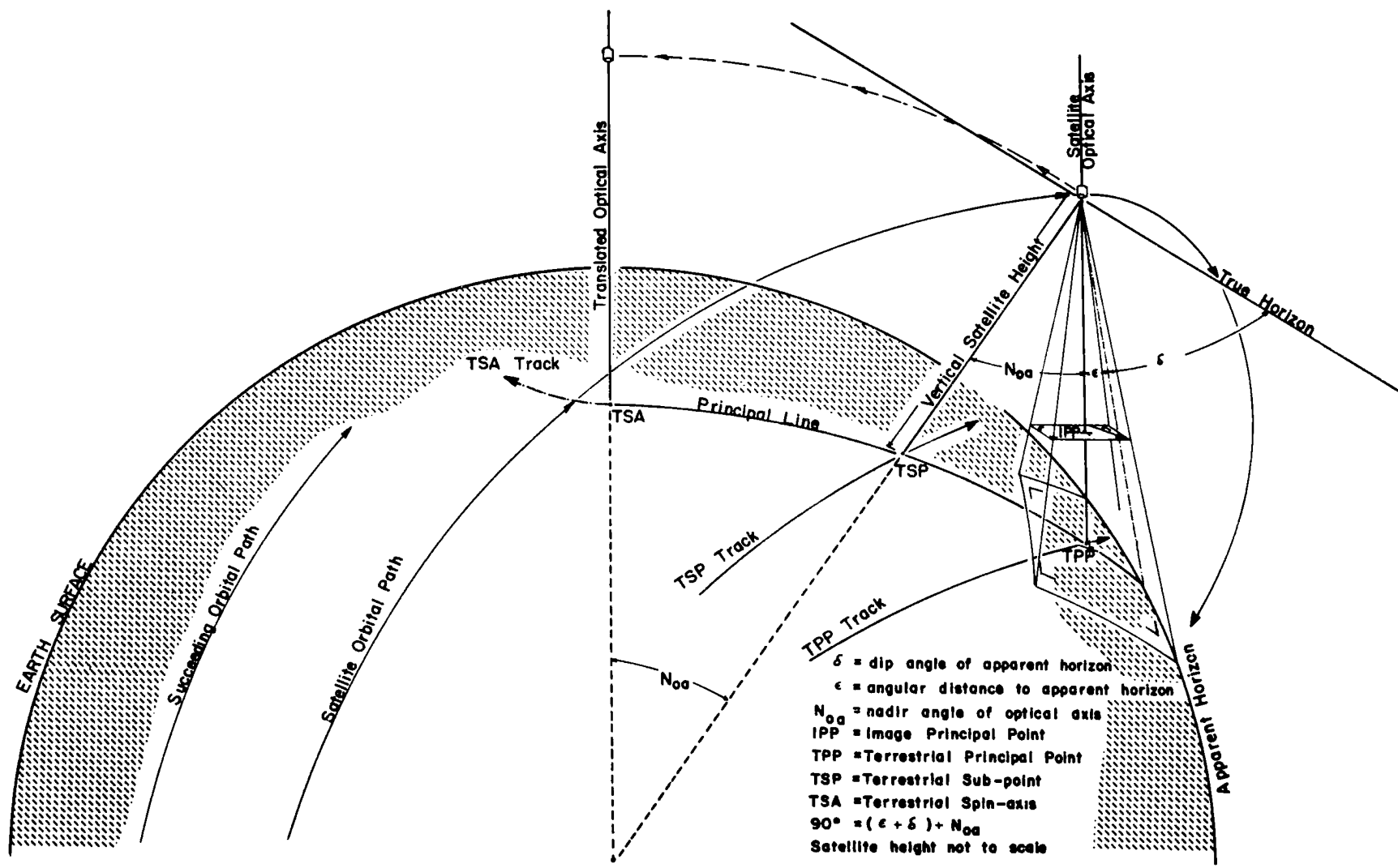may differ from the programmed time by a few seconds to a few minutes.

Fig. 1 Geometry of TIROS satellite photography. Orbital path,
image - object relationships, and point tracks are shown.
(For explanation, see text).

If there is a time error of more than 5 seconds, the corresponding errors in geographical location will be considerable, since the satellite travels a distance of approximately 250 miles in one minute.

The cameras themselves prove to have considerable lens distortion, and, together with electronic distortion, cause an error too serious to ignore. Therefore, a target is used for distortion correction prior to launch. An example of the target picture for camera 1, TIROS V, is shown in Figure 2a. From this target picture, a distortion-free grid is produced on which graphical analysis can be performed with relatively small error (see Figure 2b). One such distortion-free grid must be prepared for each TIROS camera. For direct mode readout, the word "DIRECT" is placed at the legend side of the TIROS picture. However, since the tape mode pictures are reversed during readout, the distortion-free grid when used for tape mode must be rotated 180° about the principal point; the word "TAPE" is then at the legend side of the picture.

It can be seen from Figure 1 that the earth's surface is tiltet with respect to the image plane of the camera. The angle of tilt is equal to the nadir angle of the optical axis (N_{oa}). The optical axis does not necessarily intersect the image plane at the center of the fiducial cross. This intersection, defined as the image principal point (IPP), has been located on the distortion-free grid with the aid of the target photo. The intersection of the optical axis with the earth's surface is defined as the terrestrial principal point (TPP).

If the satellite's optical axis were translated so that it intersected the earth's surface at a right angle ("Translated optical axis" in Figure 1), a spin-axis point would be located at the intersection. This point is defined as the terrestrial spin-axis point (TSA). The intersection with the earth's surface of the local vertical through the satellite (i.e. terrestrial sub-point, TSP), the TSA and the TPP lie on the same great-circle arc, called the principal line. The TPP, TSP, TSA and the earth's center lie on one plane, called the principal plane.

Fig. 2a   Pre-launch target photo-
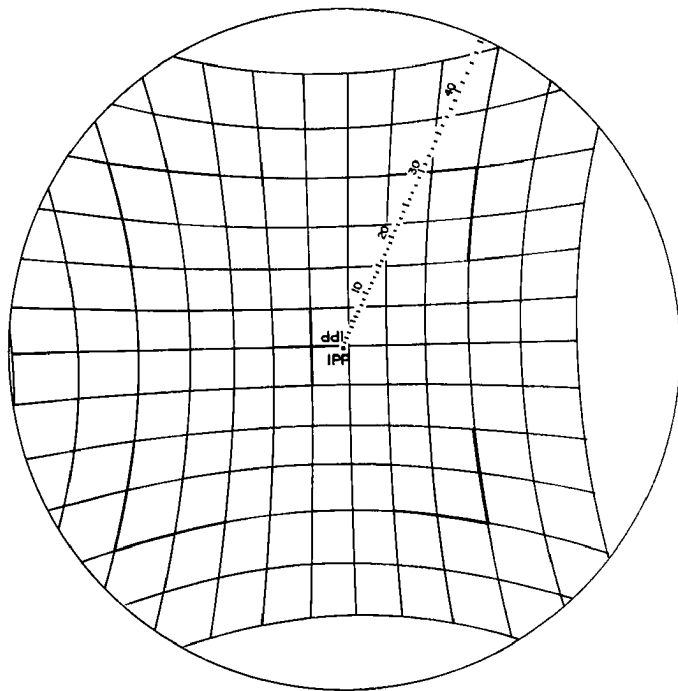graph for camera 1, TIROS V,
tape mode.
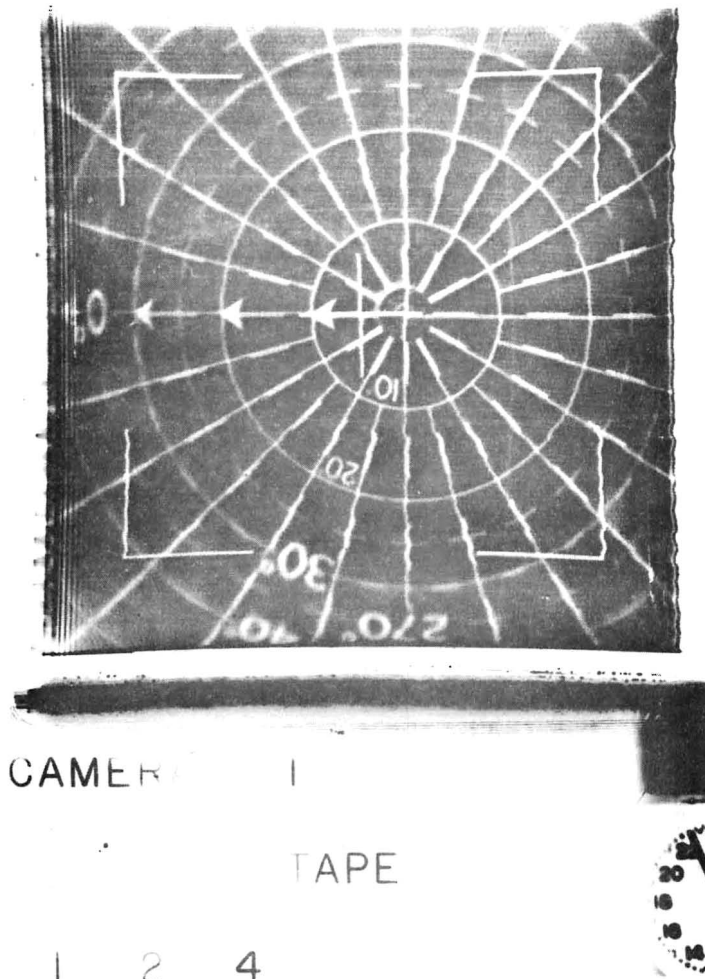
DISTORTION-FREE FIDUCIAL GRID

TIROS V

CAMERA I   DIRECT

Orbit No.

Frame No.

H =

Fig. 2b   Distortion-free grid
for camera 1, TIROS V.
The image principal point
(IPP) is entered near the
center "+" fiducial mark.
Correction is made for lens
and electronic distortions.

IPP

TAPE

Through the use of height grids and tilt grids (Figures 3a and 3b), object positions on the image plane can be located on the earth's surface. These grids can be obtained from the U. S. Department of Commerce Weather Bureau, Meteorological Satellite Laboratory, Washington, D. C. Two basic systems of gridding have been developed in connection with the rectification process. A combination grid system developed by Glaser (1960) uses uniquely defined grids which take into account both satellite height and tilt. This system has the advantage of saving time, but due to the eccentricity of the satellite orbits, requires a large library of grids. The second system (Fujita, 1961, 1963) utilizes height grids in increments of 10 kilometers and tilt grids in increments of 2 degrees. A library of 100 tilt grids (0 to 99 degrees) and 50 height grids (500 to 990 kilometers) suffices for the accuracy required in research, whereas 5000 grids would be needed for the same accuracy using combination grids. The error resulting from these finite grid increments is less if the nadir angle is small than if it is large (Fujita, 1964).

Figure 4 shows a map projection on which graphical analysis is made in connection with rectification. This <u>Oblique Equidistant Cylindrical</u> projection (OEC) is a Mercator projection wrapped obliquely around the earth. The projection equator coincides with a great circle on the earth's surface at the orbital inclination of the satellite (48.4 degrees for TIROS I through IV, and 58.3 degrees for TIROS V through VII). Great circle distances are conserved on the OEC.

Data Requirements and Sources

Satellite attitude data required for rectification and the source from which the data can be obtained are:

(1) <u>Terrestrial sub-points</u> (latitude and longitude) and <u>satellite height</u>; Meteorological Satellite Laboratory, Washington, D. C. (Table I).

HEIGHT GRID, H = 770 Km, δ=26.9°
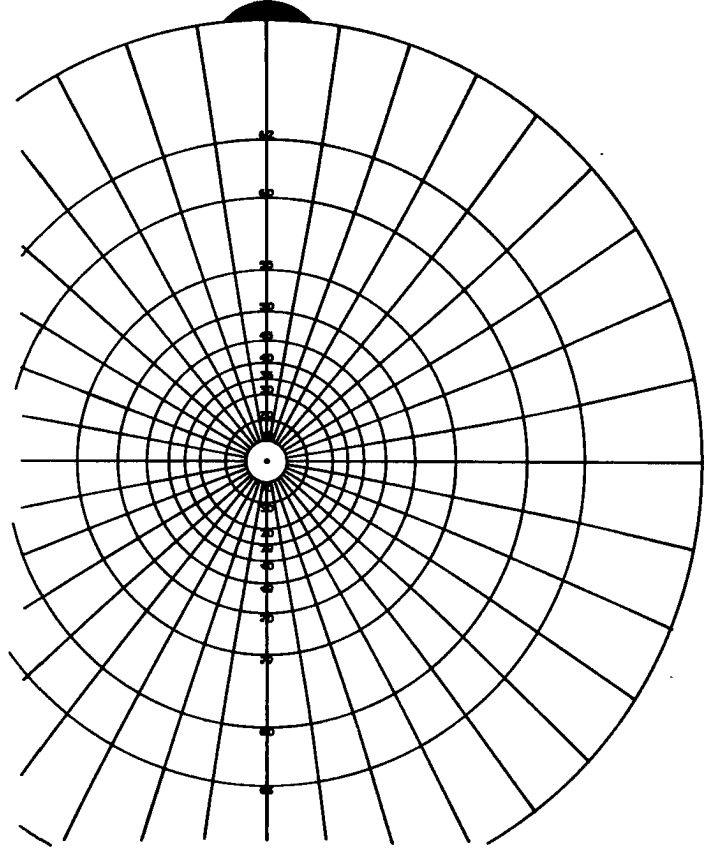
Fig. 3a Height grid for 770 km.
Dip angle is shown in upper
right hand corner. Isolines
are nadir angles and azimuths.
Scale is the same as that of
the OEC chart.

NADIR ANGLE GRID $N_{oo} = 40°$
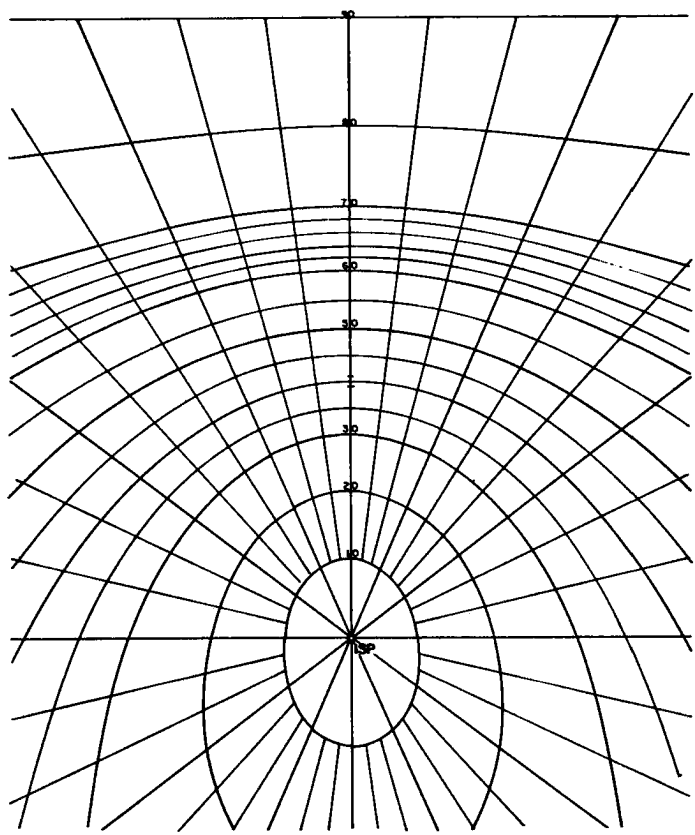
Fig. 3b Nadir angle grid for
40° tilt. Isolines are nadir
angles and azimuths.
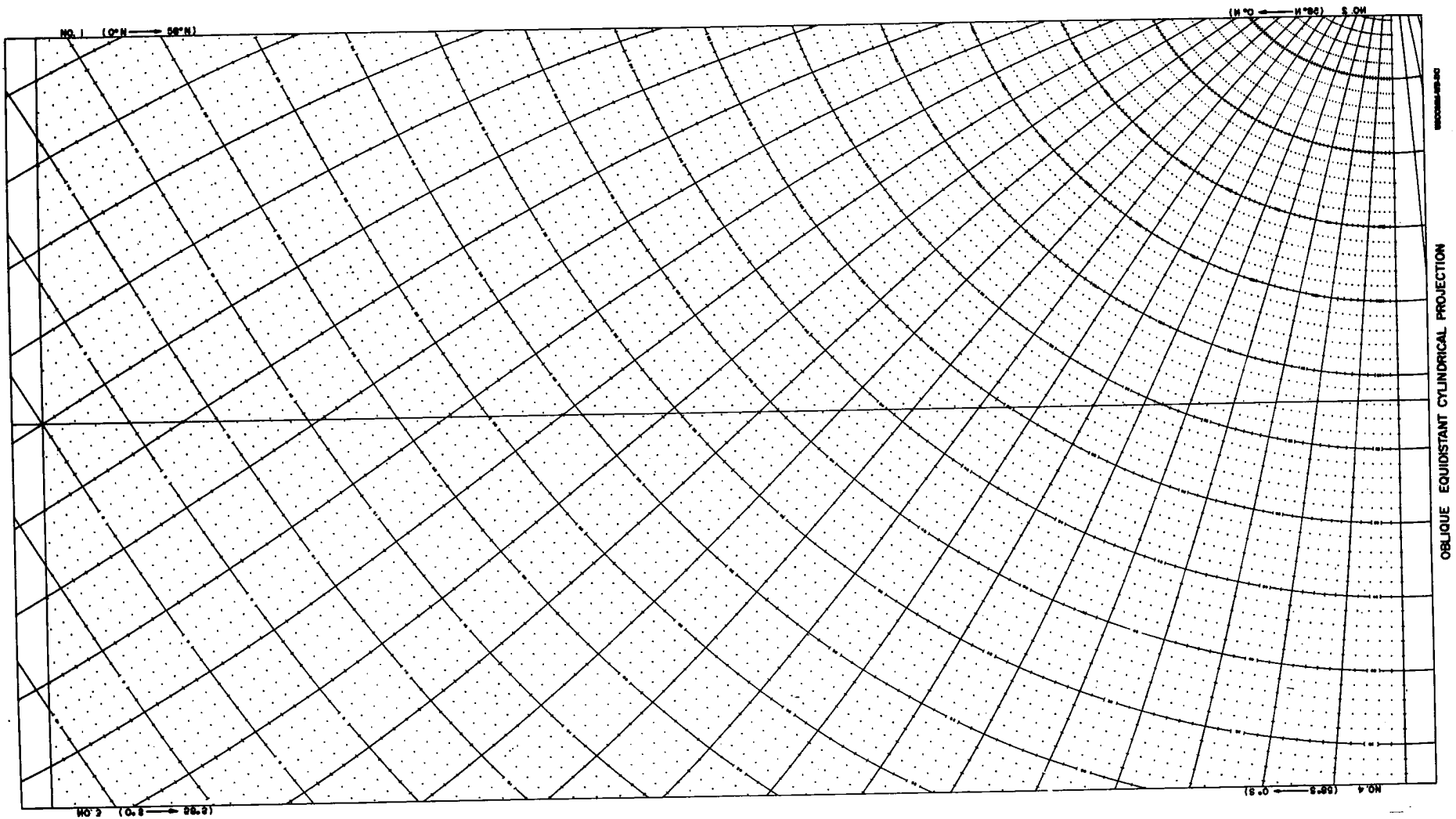
Fig. 4 Oblique equidistant cylindrical projection (OEC). The projection equator is tangent to a great circle on the earth's surface. The numbered lines designate latitude; unnumbered lines designate longitude.

Table 1: Portion of definitive attitude data sheet. Column 1, time; column 2, latitude of TSP; column 3, longitude of TSP; column 4, height in kilometers of satellite above the earth's surface. "Burst pass" is the actual picture-taking orbit number.

| DAY	TIME HR. (1)	MIN.	SATELLITE COORDINATES LAT. (2)	LONG. (3)	HGT. (4)
			BURST PASS NO. 4348		
18	19	44	1.9	W133.7	897
18	19	45	4.9	W132.2	888
18	19	46	7.8	W130.5	877
18	19	47	10.8	W128.9	867
18	19	48	13.8	W127.2	856
18	19	49	16..7	W125.5	845
18	19	50	19..7	W123.7	834
18	19	51	22.6	W121.8	823
18	19	52	25.5	W119.8	812
18	19	53	28.4	W117.7	800
18	19	54	31.2	W115.4	789
18	19	55	34.0	W113.0	778
18	19	56	36.8	W110.4	766
18	19	57	39.5	W107.6	755
18	19	58	42.1	W104.5	744
18	19	59	44.6	W101.1	733
18	20	-0	46.9	W 97.5	722
18	20	1	49.2	W 93.4	711
18	20	2	51.3	W 88.9	701
E 18	20	3	53.1	W 84.0	690
E 18	20	4	54.8	W 78.7	681
E 18	20	5	56.1	W 72.9	671
E 18	20	6	57.2	W 66.7	662
E 18	20	7	57.9	W 60.2	653

(2) <u>Celestial coordinates</u> of terrestrial spin-axis point;
    TIROS Attitude Summaries, NASA, Goddard Space
    Flight Center, Greenbelt, Maryland (Goldshlak, 1962, 1963).

(3) <u>Programmed picture time</u>; Catalogue of Meteorological
    Satellite Data, U. S. Weather Bureau, Department of
    Commerce, Washington, D. C.

GRAPHICAL PROCEDURES FOR RECTIFICATION

Picture Analysis

A distorted grid must be constructed for each sequence of
TIROS photographs. Even though minor changes in electronic
distortion may occur in the picture sequence from one picture to
the next, a mean grid for the sequence will serve. Fiducial marks
are traced from one or more photographs, and compared with, and
adjusted for, the other photographs so that a "best-fit" grid results
for the entire sequence. The center fiducial marks are extended,
and the corner L-shaped marks connected with smooth curves.
The distance between the intersections of the center extensions
and the curved outer lines is divided into four equal intervals,
Two more additional intervals are extended beyond the corners.
When these points are connected into a grid, using smooth curved
lines, a 12 X 12 - interval grid results, such as is shown in Figure 5
for TIROS V orbit 4348 tape mode. The principal point is transferred
from the distortion-free grid to the distorted grid by placing it in the
same relative position with respect to the gridding. Special care should
be taken with the orientation of the distortion-free grid, since the
tape mode is inverted with respect to the direct mode. The principal
point, however, remains in the same grid position for both direct and
tape modes.
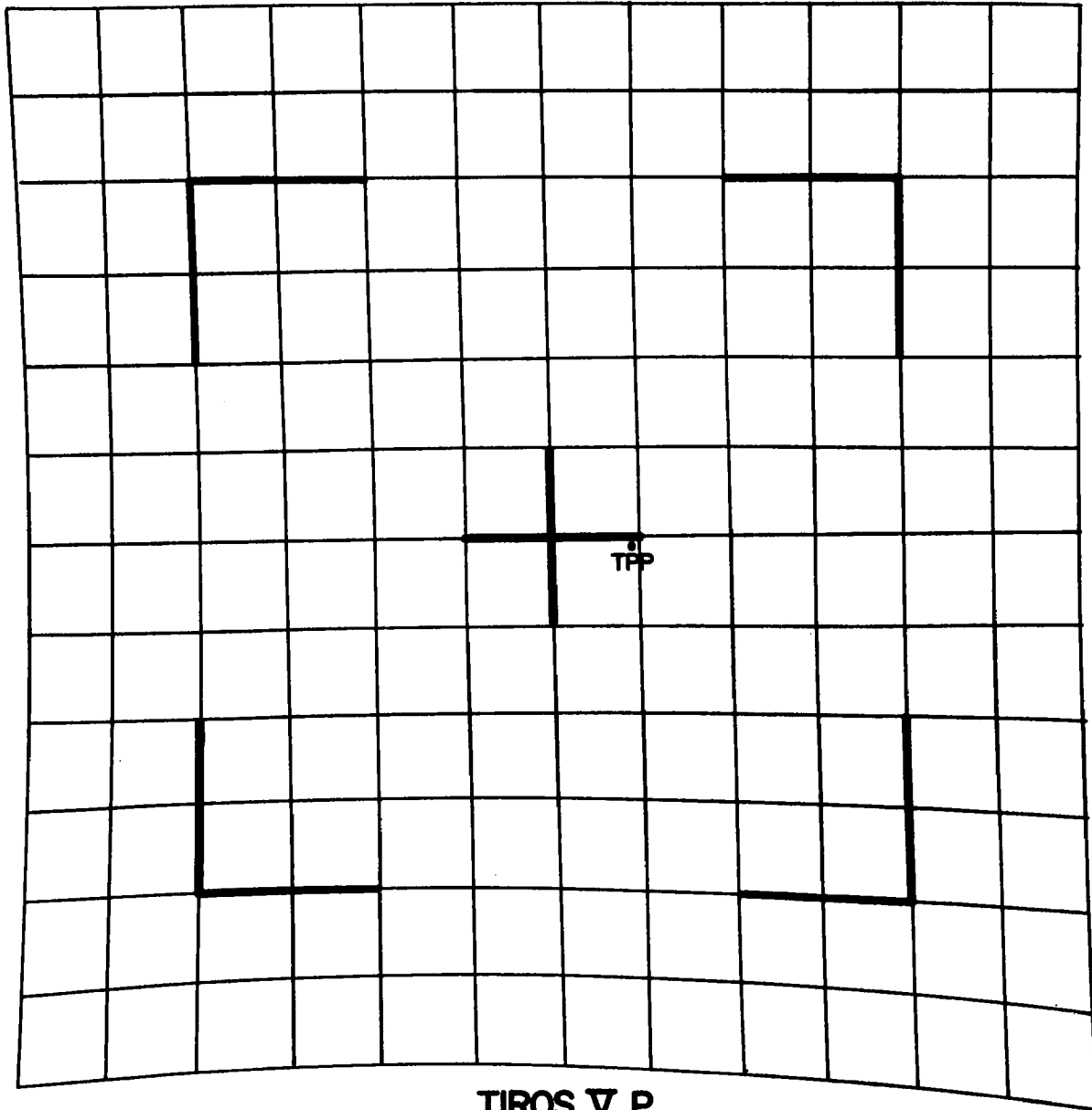
TIROS Ⅴ P
ORBIT 4348 TAPE
CAMERA I
DISTORTED GRID

Fig. 5   Mean distorted grid for TIROS V, camera 1, orbit 4349 R/0
4348.   Principal point has been transferred from the distortion-
free grid.

The principal point is transferred to each photograph, and then entered on neighboring photographs by making use of land-marks and cloud patterns as reference points (Figure 6). If the orbit is tape mode, the numbers of the frames are reversed; that is, the first photograph is numbered 32, the second 31, etc. If the orbit is direct mode, the first photograph is numbered 1, the second 2, etc. The apparent horizon, if it appears on the photograph, and the principal points are traced from each photo-graph onto a distorted grid, as shown in Figure 7a.

Since the graphical analysis cannot be made on the distorted grid, the principal points and apparent horizon must be transferred from the distorted grid to a distortion-free grid (Figures 2b and 7b) for each photograph. A line is drawn connecting the principal points, representing the track across the earth's surface made by the optical axis as the satellite orbits the earth (TPP track, dashed line in Figure 7b, connecting IPP's of frames 14, 12, 10, and 8). Since the points may deviate slightly from a smooth line, a "best-fit" line is used. The accuracy with which this line and the apparent horizon are drawn determines to a great extent the accuracy of the time corrections made for the tape modes, as well as the orientation of grids used later in the rectification process.

Using the principal point of the frame under consideration (e. g., number 14 in Figure 7b) as center, arcs are laid off on the apparent horizon in order to help find the point of closest distance on the horizon from the IPP. The straight connecting line between the IPP and this point on the horizon gives the orientation of the principal line (solid line in Figure 7b). The angular distance from the principal point to the closest horizon point is measured by means of the small scale originating at the IPP on the distortion-free grid (Figures 2b and 7b). This angle corresponds to the angle ϵ in Figure 1.
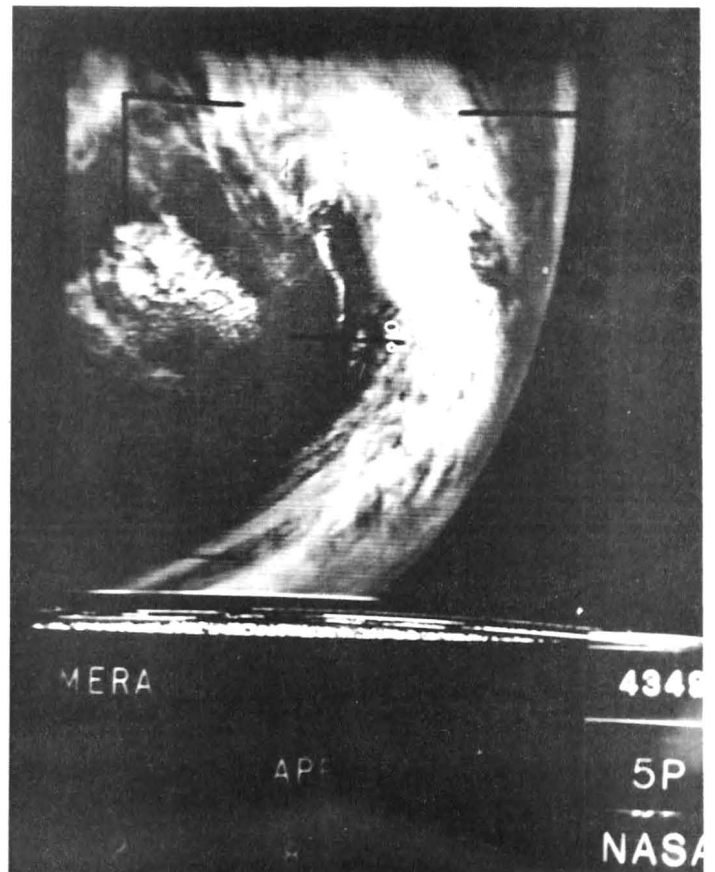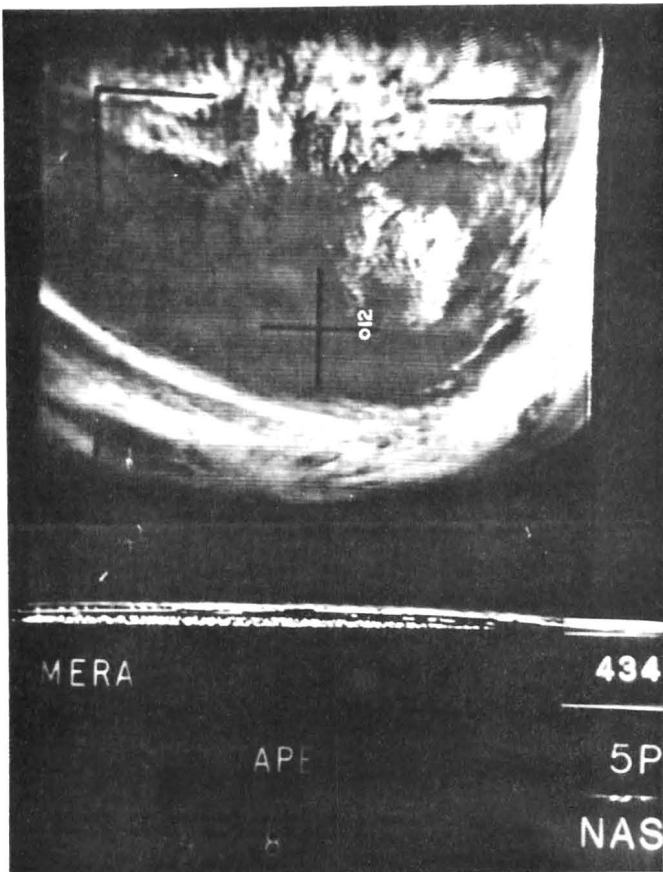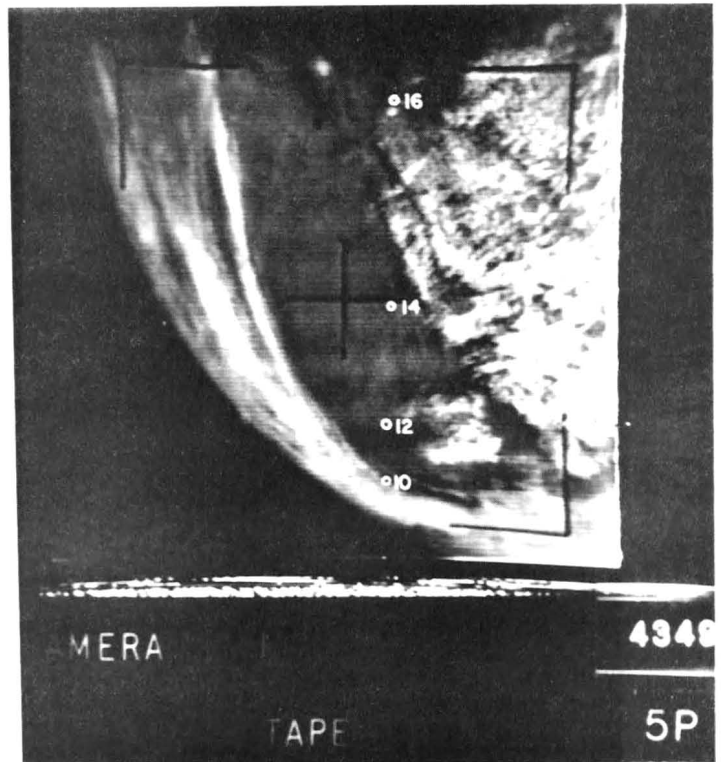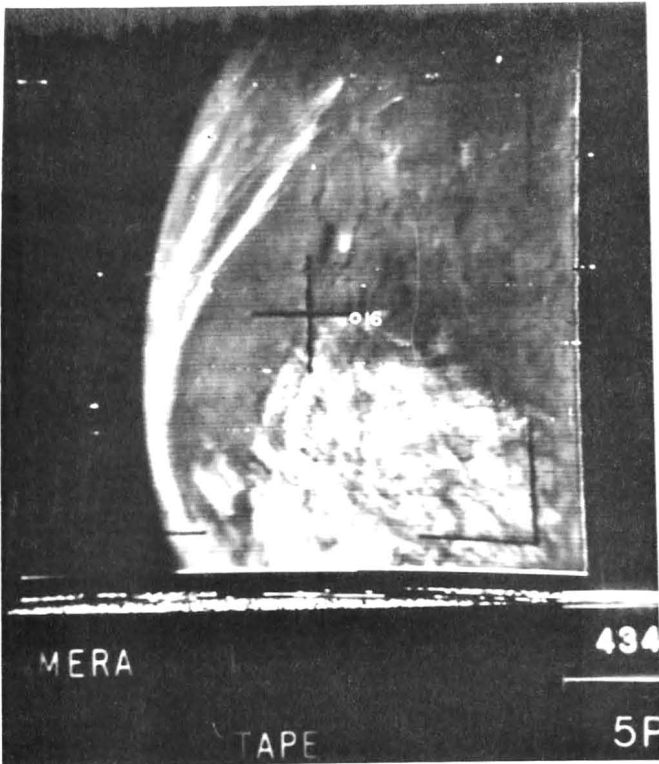
Fig. 6   Frames 10, 12, 14 and 16 TIROS V orbit 4349 R/0 4348.
The numbered circles are the principal points of the frames.

TIROS Ⅴ P
ORBIT 4348 TAPE
CAMERA I
DISTORTED GRID

Fig. 7a Mean distorted grid (see
Fig. 5a) with latitude-longi-
tude intersections plotted. The
solid curved line is the appar-
ent horizon traced from frame
14 TIROS V orbit 4349 R/0
4348.
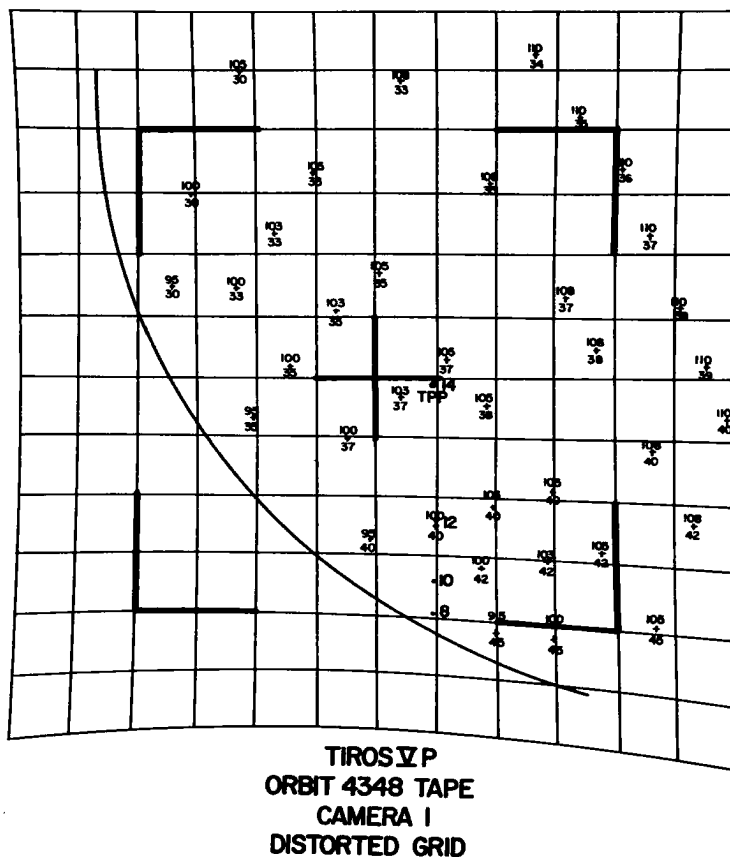
DISTORTION—FREE FIDUCIAL GRID

TIROS V

CAMERA I   DIRECT

Orbit   No. 4348T

Frame No. 14

Height   772 Km

TAPE

Fig. 7b Distortion-free grid with
apparent horizon transferred
from distorted grid. The prin-
cipal line construction is shown.
The dashed line is the IPP track;
intersections are longitude -
latitude intersections from the
OEC chart. (For explanation,
see text).

The dip angle δ between the true and apparent horizons (Figure 1) is specified on the appropriate height grid (Figure 3a). The nadir angle of the optical axis, N_{oa}, is computed for the photograph by means of the expression

$$N_{oa} = 90^{\circ} - (\epsilon + \delta).$$

The distortion-free grid is superimposed on the tilt grid whose angle is closest to the nadir angle of the optical axis (see Figure 12 b). The central azimuth on each tilt grid is marked one degree either side of the designated angle (e. g., 41° and 39° on the 40° grid shown in Figure 3b). This allows the grid to be used to the nearest degree of nadir angle. The IPP on the distortion-free grid coincides with the point on the central azimuth equal to the optical axis nadir angle of the frame under consideration, and the principal line lies along the central azimuth. The ISP of the frame coincides with the origin of the tilt grid. The curvature of the 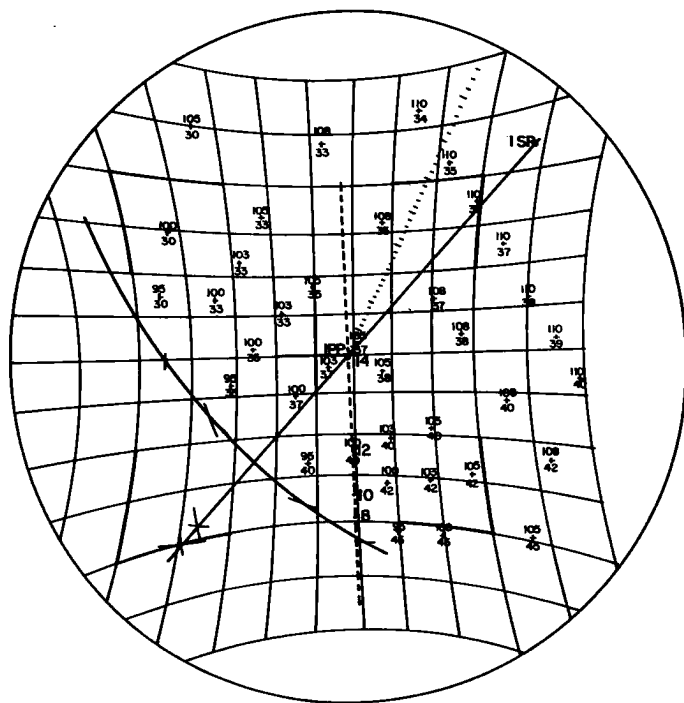apparent horizon on the distortion-free grid should agree with the curvature of the isolines of nadir angle on the tilt grid. Lack of agreement of the curves indicates an error in the analysis up to this point.

OEC Projection Chart Analysis

The celestial coordinates of the satellite spin-axis point are converted to terrestrial coordinates for a given frame time by allowing for the rotation of the earth. The celestial coordinates are given as the customary right ascension and declination in the TIROS attitude summaries. The latitude of the TSA is assumed to be equal to the declination, and to be constant for the entire picture sequence (see Figures 8, 10, and 12 a). The right ascension is related to east longitude of the TSA by the equation

$$\phi_{TSA} = \phi_{RA} - F(t)$$

where ϕ_{TSA} is the east longitude of the TSA, ϕ_{RA} the right ascension,
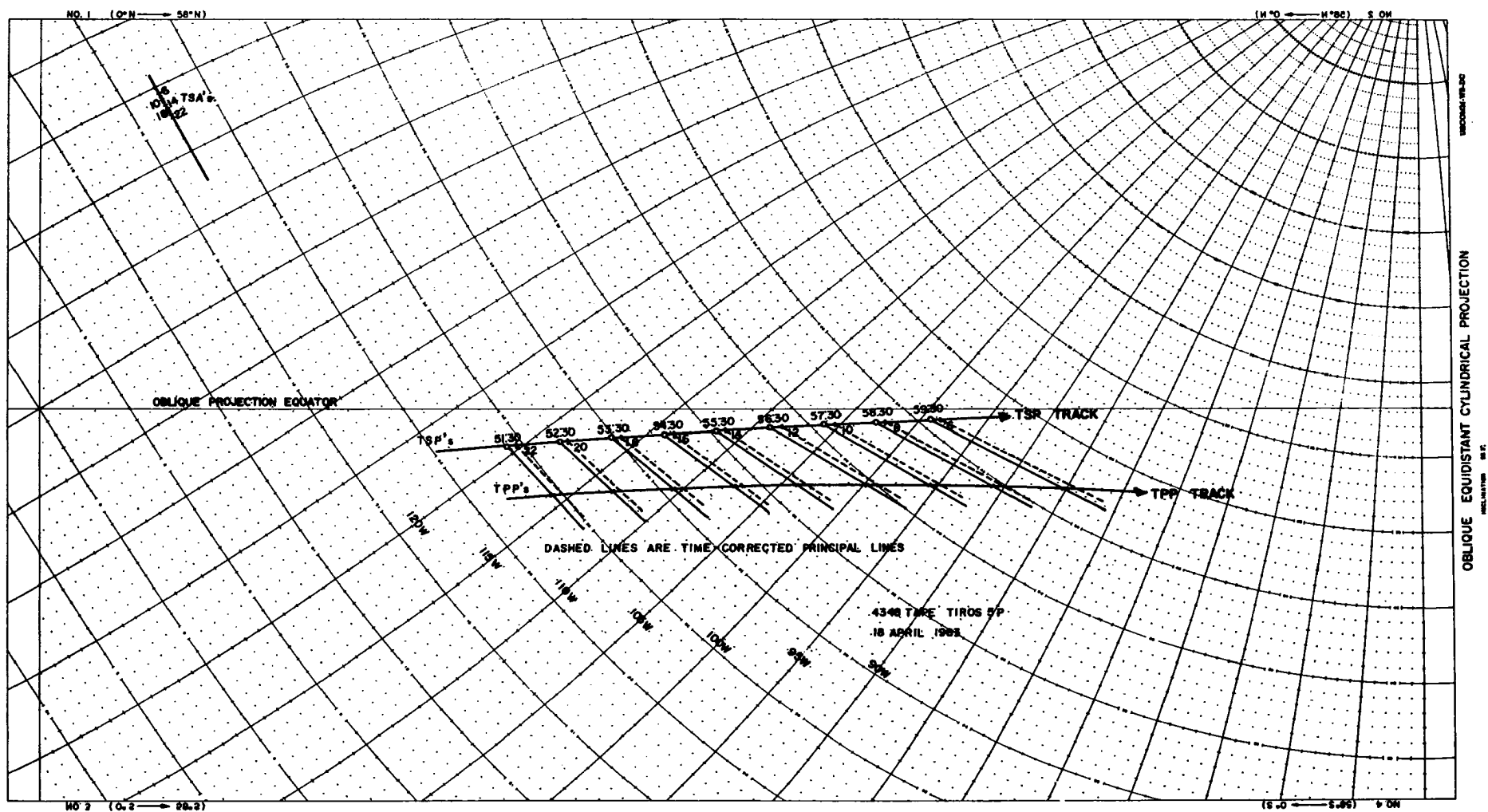
Fig. 8   Oblique equidistant cylindrical projection with TSP track,
TPP track and time-corrected principal lines (dashed lines).
The picture frame numbers are located at the corrected exposure
times on the TSP track.

and F (t) a time function.   The time function is the sum of the year, month, day, minute, and second functions, which start at 0000Z March 21 and end 2400Z March 20 of the following year.   For frame 14, TIROS V orbit 4348 tape mode, these are:

$$\phi_{RA} \quad = \quad 351.5$$

$$F\ (yr) \quad = \quad 2.21$$

$$F\ (day) \quad = \quad 27.60$$

$$F\ (hr) \quad = \quad 105.78$$

$$F\ (min) \quad = \quad 13.79$$

$$\underline{F\ (sec) \quad = \quad 0.13}$$

$$F\ (t) \quad = \quad 145.09$$

$$\phi_{TSA} \quad = \quad 153.6^{o} \quad \text{west longitude.}$$

Values for the time functions are taken from Table 2 (Fujita, 1963).

The terrestrial sub-points (TSP) for the programmed picture times are taken from Table 1, columns 2 and 3, to the nearest 0.1 degree, and heights to the nearest kilometer (column 4).   The TSP's are plotted on the OEC chart, assigning arbitrary longitude values to the meridians on this diagram to place the TSP track near the projection equator.   The TSP's are labelled with the programmed picture time, and connected with a smooth line (TSP track) as shown in Figure 8.

The spin-axis point (TSA) for the selected picture time is plotted on the OEC chart, and the TSA's for the remainder of the picture sequence determined by the formula.

$$\phi_{TSA} = \phi_{TSA,\ r} - \tfrac{1}{4}\ (t_{f} - t_{r}) \quad \text{east longitude,}$$

assuming that the latitude of the TSA remains constant.   Time t is given in minutes. ϕ_{TSA} is the longitude for a given frame, $\phi_{TSA,\ r}$ is the longitude for the reference frame (number 14 in the example), t_{f} the time of the given frame, and t_{r} the time of the reference frame.

YEAR FUNCTION

1960	1961	1962	1963	1964	1965	1966	1967	1968	1969	1970
-2.48	-1.73	-1.97	-2.21	-2.45	-1.70	-1.94	-2.18	-2.42	-1.68	-1.91

DAY FUNCTION (* is for leap year)

DAY	MAR	APR	MAY	JUN	JUL	AUG	SEPT	OCT	NOV	DEC	JAN	FEB	MAR	MAR*
1		10.84	40.41	70.96	100.53	131.08	161.64	191.21	221.76	251.33	281.88	312.44	340.03	341.02
2		11.83	41.39	71.95	101.52	132.07	162.62	192.19	222.75	252.31	282.87	313.42	341.02	342.00
3		12.81	42.38	72.93	102.50	133.06	163.60	193.18	223.73	253.30	283.85	314.41	342.00	342.99
4		13.80	43.37	73.92	103.49	134.04	164.60	194.16	224.72	254.28	284.84	315.39	342.99	343.97
5		14.78	44.35	74.91	104.47	135.03	165.58	195.15	225.70	255.27	285.82	316.38	343.97	344.96
6		15.77	45.34	75.89	105.46	136.01	166.57	196.13	226.69	256.26	286.81	317.36	344.96	345.95
7		16.76	46.32	76.88	106.44	137.00	167.55	197.12	227.67	257.24	287.80	318.35	345.95	346.93
8		17.74	47.30	77.86	107.43	137.98	168.54	198.11	228.66	258.23	288.78	319.33	346.93	347.92
9		18.73	48.29	78.85	108.42	138.97	169.52	199.09	229.64	259.21	289.77	320.32	347.92	348.90
10		19.71	49.28	79.83	109.40	139.96	170.51	200.08	230.63	260.20	290.75	321.31	348.90	349.89
11		20.70	50.26	80.82	110.39	140.94	171.49	201.06	231.62	261.18	291.74	322.29	349.89	350.87
12		21.68	51.25	81.80	111.37	141.93	172.48	202.05	232.60	262.17	292.72	323.28	350.87	351.86
13		22.67	52.24	82.79	112.36	142.91	173.46	203.03	233.59	263.16	293.71	324.26	351.86	352.84
14		23.65	53.22	83.78	113.34	143.90	174.45	204.02	234.57	264.14	294.69	325.25	352.84	353.83
15		24.64	54.21	84.76	114.33	144.88	175.44	205.00	235.56	265.13	295.68	326.23	353.83	354.82
16		25.63	55.19	85.75	115.32	145.87	176.42	205.99	236.54	266.11	296.67	327.22	354.82	355.80
17		26.61	56.18	86.73	116.30	146.85	177.41	206.98	237.53	267.10	297.65	328.20	355.80	356.79
18		27.60	57.16	87.72	117.29	147.84	178.39	207.96	238.52	268.08	298.64	329.19	356.79	357.77
19		28.58	58.15	88.70	118.27	148.83	179.38	208.95	239.50	269.07	299.62	330.18	357.77	358.76
20		29.57	59.14	89.69	119.26	149.81	180.36	209.93	240.49	270.05	300.61	331.16	358.76	359.74
21	0.00	30.55	60.12	90.68	120.24	150.80	181.35	210.92	241.47	271.04	301.59	332.15		
22	0.99	31.53	61.11	91.66	121.23	151.78	182.34	211.90	242.46	272.03	302.58	333.13		
23	1.97	32.52	62.09	92.65	122.21	152.77	183.32	212.89	243.44	273.01	303.56	334.12		
24	2.96	33.51	63.08	93.63	123.20	153.75	184.31	213.88	244.43	274.00	304.55	335.10		
25	3.94	34.50	64.06	94.62	124.19	154.74	185.29	214.86	245.41	274.98	305.54	336.09		
26	4.93	35.48	65.05	95.60	125.17	155.72	186.28	215.85	246.40	275.97	306.52	337.08		
27	5.91	36.47	66.04	96.59	126.16	156.71	187.26	216.83	247.39	276.95	307.51	338.06		
28	6.90	37.45	67.02	97.57	127.14	157.70	188.25	217.82	248.37	277.94	308.49	339.05		
29	7.88	38.44	68.01	98.56	128.13	158.68	189.24	218.80	249.36	278.92	309.48	340.03		
30	8.87	39.42	68.99	99.55	129.11	159.67	190.22	219.79	250.34	279.91	310.46			
31	9.85		69.97		130.10	160.65		220.77		280.90	311.45			

HOUR FUNCTION (hours in Greenwich time)

0	1	2	3	4	5	6	7	8	9	10	11
-180.00	-164.96	-149.92	-134.88	-119.84	-104.79	-89.75	-74.71	-59.67	-44.63	-29.59	-14.55

12	13	14	15	16	17	18	19	20	21	22	23
00.49	15.53	30.58	45.62	60.66	75.70	90.74	105.78	120.82	135.86	150.90	165.94

MINUTE FUNCTION

0	1	2	3	4	5	6	7	8	9	10	11	12	13	14	15	16	17	18	19
0.00	0.25	0.50	0.75	1.00	1.25	1.50	1.75	2.01	2.26	2.51	2.76	3.01	3.26	3.51	3.76	4.01	4.26	4.51	4.76

20	21	22	23	24	25	26	27	28	29	30	31	32	33	34	35	36	37	38	39
5.01	5.26	5.51	5.77	6.02	6.27	6.52	6.77	7.02	7.27	7.52	7.77	8.02	8.27	8.52	8.77	9.02	9.28	9.53	9.78

40	41	42	43	44	45	46	47	48	49	50	51	52	53	54	55	56	57	58	59
10.03	10.28	10.53	10.78	11.03	11.28	11.53	11.78	12.03	12.28	12.53	12.78	13.04	13.29	13.54	13.79	14.04	14.29	14.54	14.79

SECOND FUNCTION

0	2	4	6	8	10	12	14	16	18	20	22	24	26	28	30	32	34	36	38	40	42	44	46	48	50	52	54	56	58	60
0.00	0.01	0.02	0.03	0.04	0.04	0.05	0.06	0.07	0.08	0.08	0.09	0.10	0.11	0.12	0.13	0.13	0.14	0.15	0.16	0.17	0.18	0.18	0.19	0.20	0.21	0.22	0.23	0.23	0.24	0.25

Table 2 Time functions for right ascension of Greenwich (from Fujita, 1963). The sum of the individual time values is the right ascension for the time of the frame used as reference.

The azimuth and nadir angle overlay (Figure 9a), construction and geometry of which is shown in Figure 9b, is used to locate the terrestrial primary points (TPP's) on the OEC chart. The TSP of the frame under consideration is placed at the origin of the overlay, with the projection equator of the overlay approximately along the OEC projection equator. The overlay may be rotated a few degrees about the TSP without causing excessive error (Fujita, 1964). The overlay is rotated until the TSA for the frame under consideration lies on an azimuth line of the overlay. This azimuth represents the principal line, and is drawn from the TSA and extended through the TSP (Figure 10).

The great-circle distance along the azimuth from TSA to TSP, measured on the overlay, is recorded on a data sheet (Table 3) as the programmed time nadir angle for the frame. The appropriate height grid is superimposed on the OEC chart with its origin at the TSP of the frame. The TPP is located on the principal line at the point at which the height grid nadir angle is equal to the nadir angle of the optical axis. When the TPP's for each frame have been located, they are connected with a smooth line to form the TPP track.

The programmed time nadir angles obtained from the OEC chart are plotted versus programmed time as shown in Figure 11a, and the points connected with a smooth line. Using the same scale for angle versus time, the picture nadir angles are plotted against frame number, and connected with a smooth line (Figure 11b), using the same slope of line as used in the angle versus time graph. Considerably more scatter about this second line may be expected, so that care must be taken to get the best fit. These two nadir angle graphs are superimposed so that the lines coincide, and the actual time is located on the abscissa of the picture-nadir-angle-versus-frame graph (Figure 11b). If the error in time is greater than 4 or 5 seconds, a new TSP is located on the TSP track for each frame, a new principal line interpolated (dashed lines on Figure 8), and new TPP points located on the TPP track. Only if
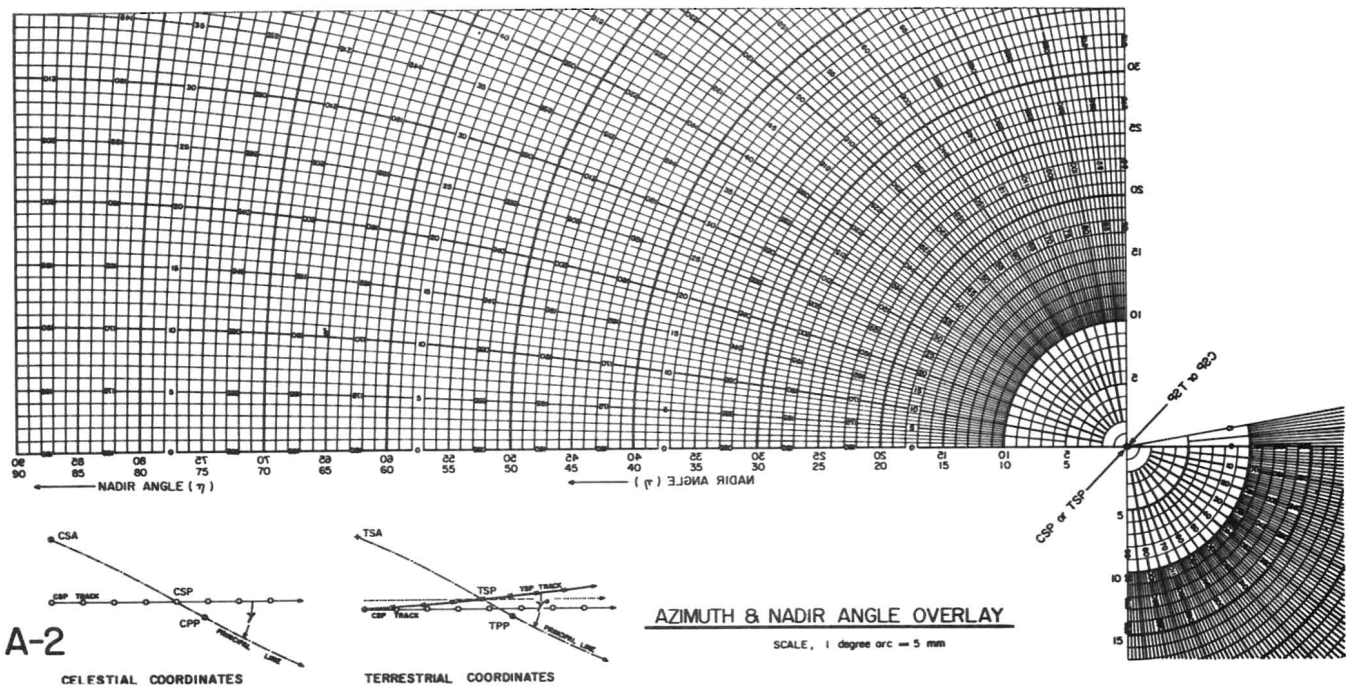
Fig. 9a Azimuth and nadir angle overlay. The isolines are of
nadir angles (values are in degrees of great-circle arc) and
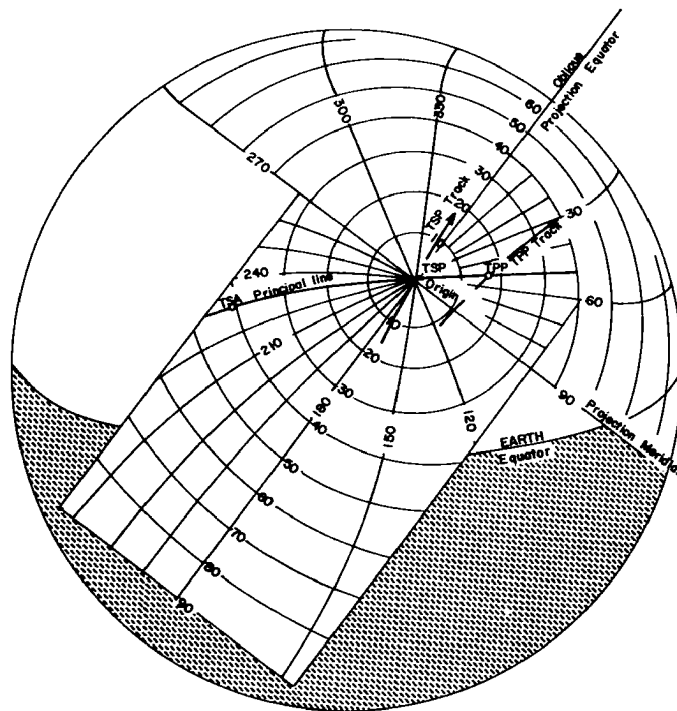azimuth.

Fig. 9b Azimuth and nadir angle overlay construction and geometry.
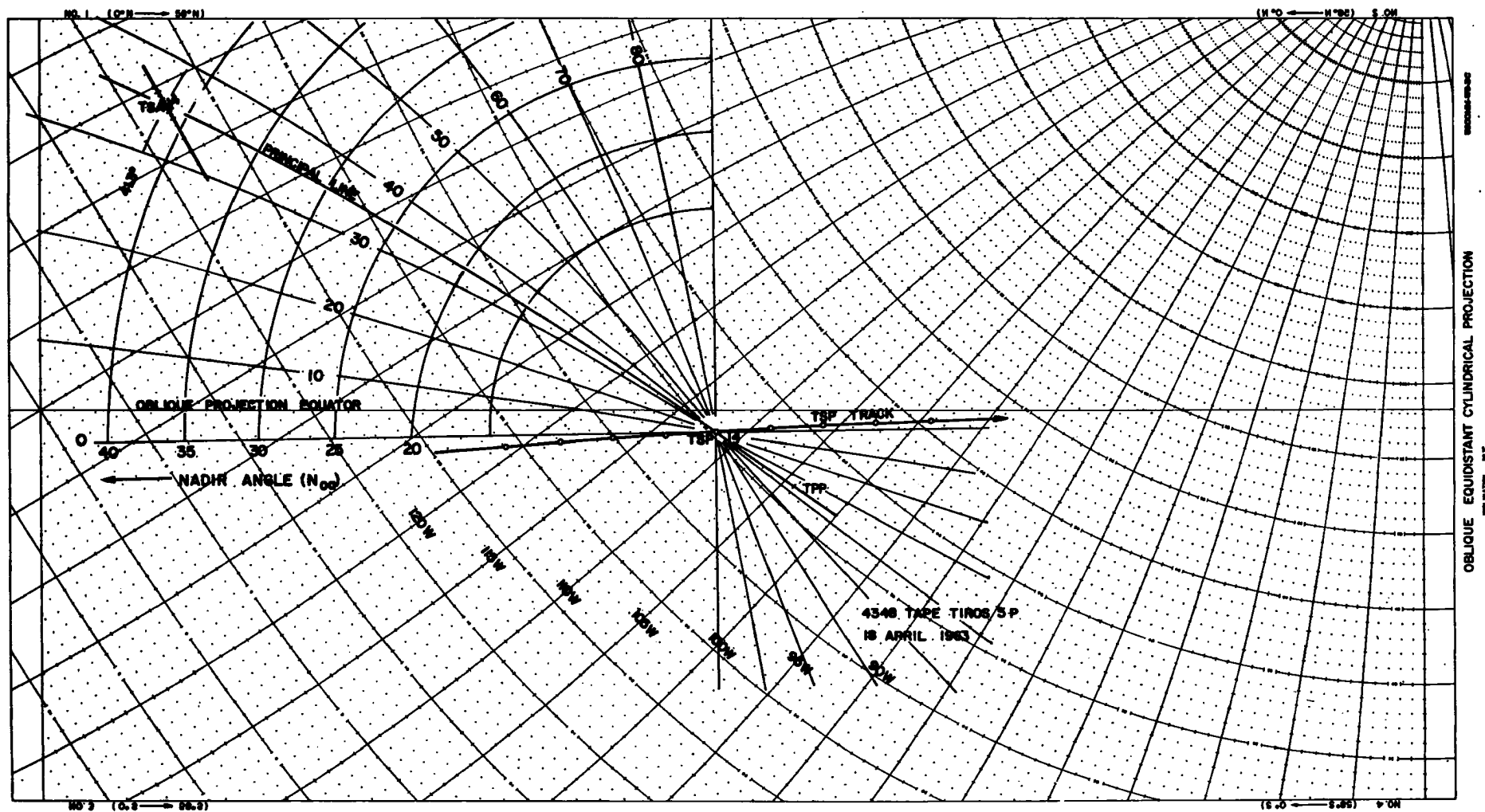Isolines are of nadir angles and azimuths. Drawing is not to
scale.

Fig. 10   Oblique equidistant cylindrical (OEC) projection superimposed
on the azimuth and nadir angle overlay. The principal line is
extended along an azimuth from the TSA through the TSP to
locate the TPP.

Table 3: Tabulation of data for TIROS V orbit 4349 R/O 4348, 18 April 1963

TIROS VP Tape Orbit 4348   18 April 1963

Frame Number	Programmed Time (GMT)	Corrected Time (GMT)	Terrestrial N. Lat.	Sub-Point W. Long.	Height Km	Nadir Angle Picture	Nadir Angle OEC Chart
24	19:50:30	19:50:40	21.1	122.8	828		
23	19:51:00		22.6	121.8	823		
22	19:51:30	19:51:40	24.1	120.8	817		30.6
21	19:52:00		25.5	119.8	812		
20	19:52:30	19:52:40	27.0	118.8	806		33.0
19	19:53:00		28.4	117.7	800		
18	19:53:30	19:53:40	29.8	116.6	795	36.2	35.6
17	19:54:00		31.2	115.4	789		
16	19:54:30	19:54:40	32.6	114.2	783	39.1	38.5
15	19:55:00		34.0	113.0	778		
14	19:55:30	19:55:40	35.4	111.7	772	41.0	41.3
13	19:56:00		36.8	110.4	766		
12	19:56:30	19:56:40	38.1	109.0	760	44.5	44.5
11	19:57:00		39.5	107.6	755		
10	19:57:30	19:57:40	40.8	106.1	750	48.0	47.5
9	19:58:00		42.1	104.5	744		
8	19:58:30	19:58:40	43.3	102.8	738	51.2	50.4
7	19:59:00		44.6	101.1	733		
6	19:59:30	19:59:40	45.8	99.3	728		53.6
5	20:00:00		46.9	97.5	722		

CELESTIAL COORDINATES FRAME 14   RA SA 351.5   DECL SA 17.0

TIME FUNCTIONS

YEAR	-2.21	351.5	360.0
DAY	27.60	-145.1	-206.4
HOUR	105.78	206.4 E	153.6 W
MINUTE	13.79		
SECOND	0.13		
	145.09		

ϕ TSA, 14 = 153.6 West Longitude

Θ TSA, 14 = 17.0 North Latitude
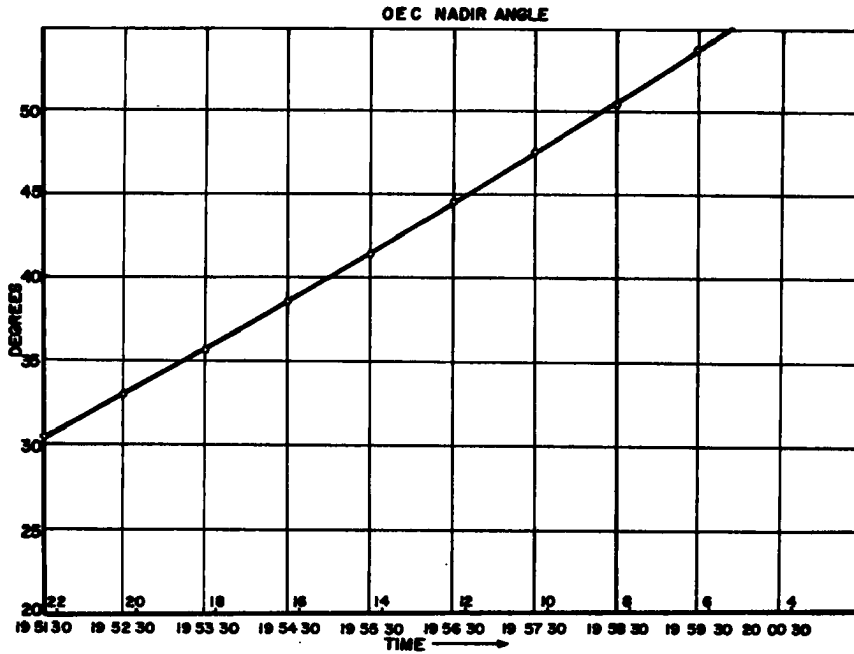
Ascending Node 134.72 W at 19:43:24 GMT

Fig. 11a Graph of programmed picture-taking times (abscissa)
versus nadir angle (ordinate). Values are taken from the OEC
chart by means of the azimuth and nadir angle overlay. The
picture frame numbers are entered on the abscissa at the cor-
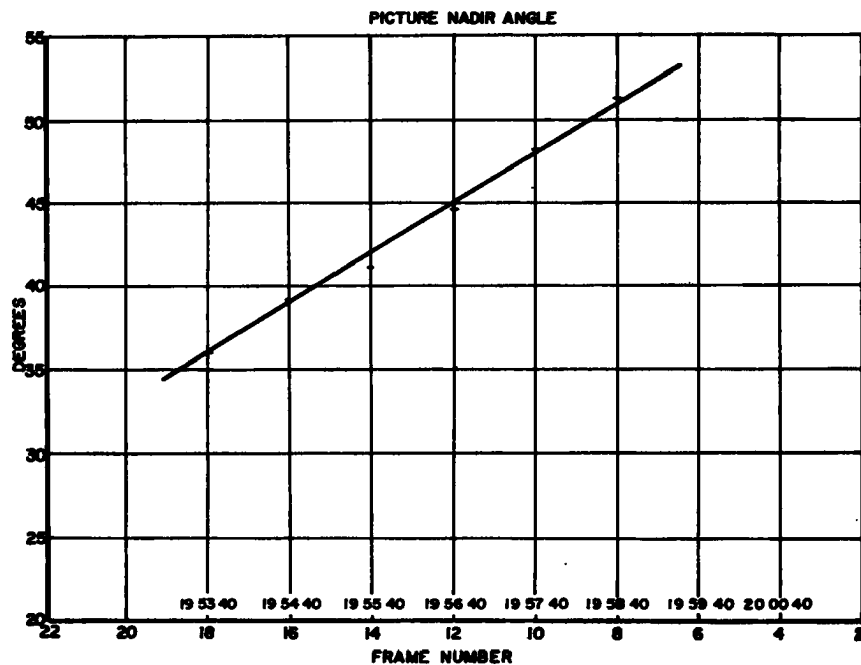rected exposure times.

Fig. 11b Graph of picture frame numbers (abscissa) versus nadir
angle (ordinate). The nadir angles are taken from the photo-
graphs. The corrected exposure times are entered on the
abscissa.

time errors on the order of minutes are found is it necessary to go back to the OEC chart and compute new tracks and graphs. The new points are then numbered with the picture frame number. If the readout is by direct mode, the nadir angle graphs need not be prepared, since the time is assumed to be correct.

Mapping of Points

The appropriate height grid (Figure 3a) is positioned on the OEC chart with its origin on the TSP of the frame to be rectified, with the center azimuth approximately parallel to the OEC projection equator, and one of the azimuth lines along the principal line (Figure 12a).

The distortion-free grid is superimposed on the nadir angle (tilt) grid corresponding closest to the frame nadir angle (Figure 12b). The distortion-free grid IPP is placed on the intersection of the frame nadir angle and the principal line of the nadir angle grid. The ISP is placed at the origin of the grid. The distortion-free grid is rotated slightly about the IPP until the IPP track (dashed line on Figure 12b) agrees in grid orientation with the TPP track on the OEC (Figure 12a). Good agreement of the tracks and principal points with regard to the respective grids is a check on the accuracy of the procedures up to this point. The slight rotation of the distortion-free grid does not cause an appreciable error (Fujita, 1964).

Intersection points of latitude and longitude are transferred from the OEC chart to the distortion-free grid, as shown on Figure 7b. The number of points transferred depends upon the accuracy requirements; points nearest the TSP point may be taken as close as every degree if desired. For less accurate analysis requirements five degree intervals may suffice. When these intersections have been transferred to the distorted grid, as shown in Figure 7a, smoothed lines are drawn for latitude and longitude lines. The smoothed lines again are those of best fit for the intersections plotted, and additional lines may be interpolated if one-degree intervals are desired. The
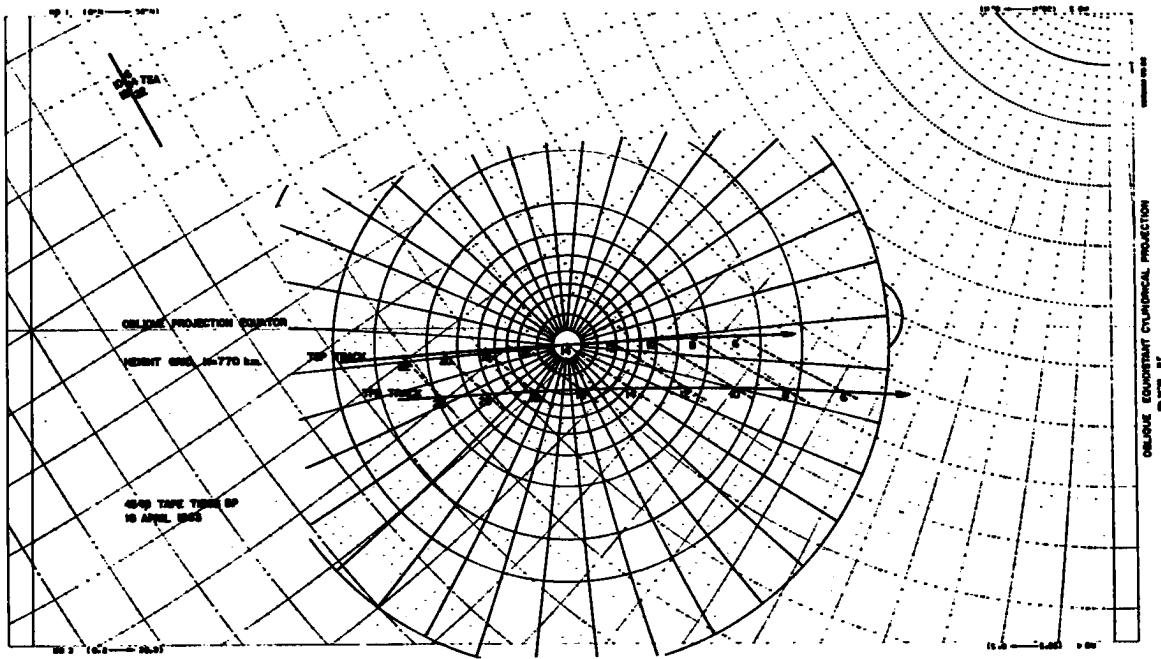
Fig. 12a Height grid superimposed on OEC chart. The corrected
principal line lies along an azimuth of the height grid; the origin
coincides with the TSP of the frame under consideration.
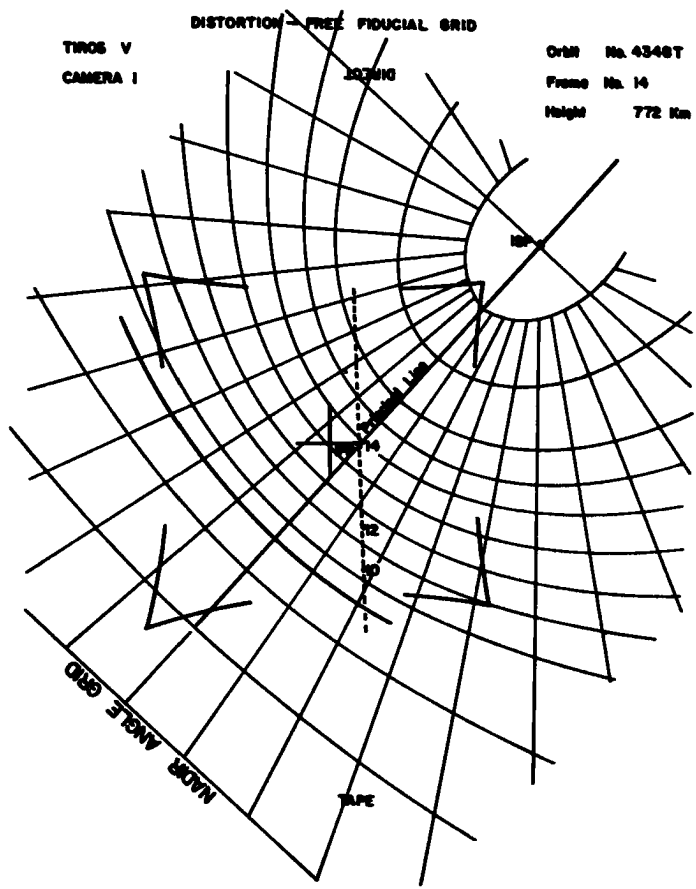

Fig. 12b Distortion-free grid
superimposed on tilt grid.
The dashed line is the IPP
track; the solid curved line
is the apparent horizon.

final rectification grid for frame 14 TIROS V orbit 4348 tape mode is shown in Figure 13. Table 3 is a suggested format for recording data extracted from the pictures and original data sources.

The rectification process fundamentally consists of four steps: (1) analysis and extraction of apparent horizons and principal points from the pictures, (2) construction of the OEC projection chart, (3) time correction determination (if tape mode), and, (4) transfer of latitude-longitude intersections to the distorted grid.

The graphical method allows several checks on the process. If the apparent horizon does not conform to the curvature on the tilt grid, if a point on a track or graph shows a large departure from the line, or if the IPP points do not agree on the OEC chart and distortion-free grids, the analysis should be checked up to that point for errors.

The grid location of geographical features determines the final accuracy of the rectification. With the aid of prepared maps of terrestrial features (Cronin, 1963), systematic errors in the analysis can be found if they exist. After having acquired some experience in rectification, the analyst will not find it difficult to translate subpoints along the TSP track in order to correct such systematic errors. This represents a considerable saving in time as compared to the mapping over of landmarks from the pictures to the OEC chart (Fujita, 1963), since a majority of the rectified pictures will not need to be corrected.
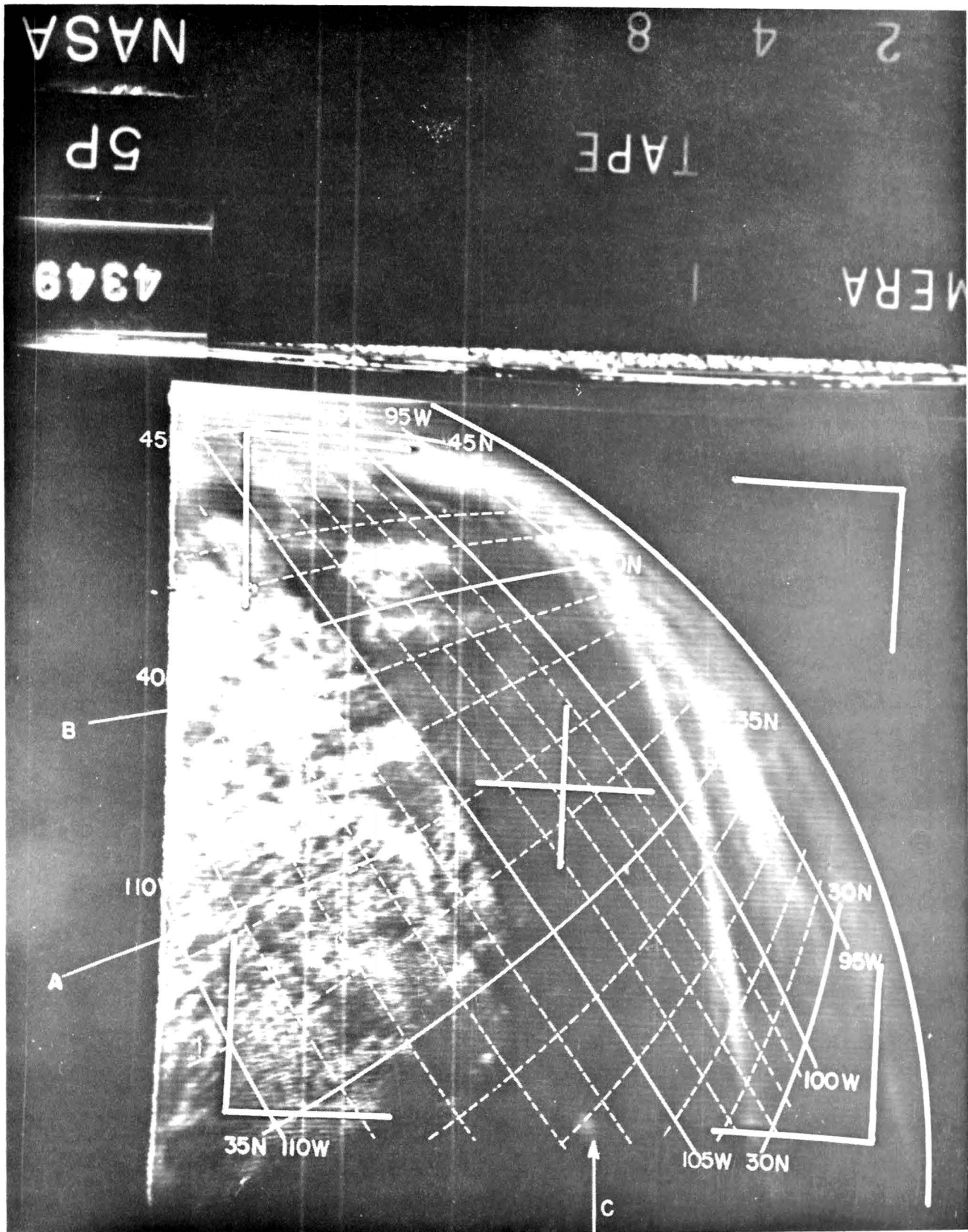
ACKNOWLEDGEMENTS

Fig. 13 TIROS photograph with latitude-longitude lines super-
imposed. Geographic features are (A) San Juan Mountains
(B) Pikes Peak, and (C) White Sands (New Mexico). The
photograph is frame 14, TIROS V, orbit 4349 R/O 4348.

GLOSSARY

DECLINATION (DEC): The angular distance of an object north or south from the celestial equator measured along the hour circle (meridian) passing through the object.

DIP ANGLE (δ): The vertical angle between the true and apparent horizons.

DISTORTED GRID: Grid designed to fit lens and electronic distortions.

DISTORTION-FREE GRID: The image of a fiducial grid adjusted to remove lens and electronic distortions.

EQUIDISTANT CYLINDRICAL PROJECTION (OEC): A Mercator projection with projection equator inclined with respect to the earth's equator.

FIDUCIAL MARKS: Index marks inscribed on vidicon system.

HEIGHT GRID: A system of azimuth and nadir angle lines on a plane surface tangent to the earth's surface.

HORIZON DISTANCE (ϵ): The radial angle between the principal point and the apparent horizon.

IMAGE PRINCIPAL POINT (IPP): The intersection of the optical axis with the image plane.

IMAGE SUBSATELLITE POINT (ISP): The intersection of the local vertical passing through the satellite with the image plane.

OPTICAL AXIS: A straight line passing through the front and rear nodal points of the camera lens.

RIGHT ASCENSION ($\emptyset_{RA}$): The arc measured eastward along the celestial equator from the vernal equinox to the great circle passing through the celestial poles and the object projected on the celestial sphere.

TERRESTRIAL PRINCIPAL POINT (TPP): The point of intersection of the optical axis of the camera with the earth's surface.

TERRESTRIAL SPIN-AXIS POINT (TSA): The point at which lines parallel to the satellite spin-axis intersects the earth's surface at right angles.

TERRESTRIAL SUBSATELLITE POINT (TSP): The point of inter-
section of the local vertical passing through the satellite with
the earth's surface.

TILT: The angle between the camera optical-axis and the local
vertical. This angle is the same as the nadir angle of the
optical-axis (N_{oa}).

TILT GRID: A grid consisting of isolines of nadir angles and
azimuths.

REFERENCES

Cronin, J. F., 1963: Terrestrial Features of the United States as
viewed by TIROS. Scientific Report No. 2, Aracon Geophysics Co.

Dean, C., Reprinted 1964: Attitude Determination from TIROS
Photographs. Aracon Geophysics Co.

Fujita, T., 1961: Outline of a Technique for Precise Rectification
of Satellite Cloud Photographs. Research Paper No. 3,
Mesometeorology Project, University of Chicago.

_____, 1963: A technique for Precise Analysis of Satellite
Photographs. Research Paper No. 17, Mesometeorology
Project, University of Chicago.

_____, 1964: Evaluation of Errors in the Graphical Rectification
of Satellite Photographs. Research Paper No. 30, Meso-
meteorology Project, University of Chicago.

Glaser, A. H., 1960: A system for the Meteorological Use Satellite
Television Observations. GRD Research Notes No. 36,
Geophysical Research Directorate.

Goldshlak, L., 1963: TIROS V Attitude Summary. Third Technical
Summary Report, Aracon Geophysics Co.

_____, 1963: TIROS VI Attitude Summary. Fourth Technical
Summary Report. Aracon Geophysics Co.

Hubert, L., 1961: TIROS I: Camera Attitude Data, Analysis of Location
Errors, and Derivation of Correction for Calibration. MSL Report
No. 5, Meteorological Satellite Laboratory.